Condensed Matter Physics, 2005, Vol. 8, No. 1(41), pp. 135–148

CONDENSED MATTER PHYSICS

On the thermodynamic properties of the generalized Gaussian core model

B.M.Mladek [1,2] , M.J.Fernaud [1] , G.Kahl [1] , M.Neumann [2]

[1] Center for Computational Materials Science
and Institut für Theoretische Physik,
Technische Universität Wien,
Wiedner Hauptstraße 8–10, A–1040 Wien, Austria

[2] Institut für Experimentalphysik,
Universität Wien,
Strudlhofgasse 4, A–1090 Wien, Austria

Received November 24, 2004

We present results of a systematic investigation of the properties of the generalized Gaussian core model of index n. The potential of this system interpolates via the index n between the potential of the Gaussian core model and the penetrable sphere system, thereby varying the steepness of the repulsion. We have used both conventional and self-consistent liquid state theories to calculate the structural and thermodynamic properties of the system; reference data are provided by computer simulations. The results indicate that the concept of self-consistency becomes indispensable to guarantee excellent agreement with simulation data; in particular, structural consistency (in our approach taken into account via the zero separation theorem) is obviously a very important requirement. Simulation results for the dimensionless equation of state, $\beta P/\varrho$, indicate that for an index-value of 4 a clustering transition, possibly into a structurally ordered phase might set in as the system is compressed.

Key words: *soft matter, integral equations, computer simulations, clustering transition, Gaussian core model*

PACS: *61.20.Gy, 61.20.Ja, 64.10.+h*

1. Introduction

Soft matter physics has become a rapidly developing, and challenging field for both experimentalists and theoreticians. For several reasons, particular effort has been made in recent years to investigate this topic. From the applied viewpoint, soft matter – bean ubiquitous in our daily life – plays a key role in many technological applications and processes. From the academic point of view, it offers a broad range of possibilities where experiment and theory can cooperate in a very constructive and complementary manner. Typical examples for soft matter systems are suspensions of mesoscopic particles (their size ranging from 1 μm to 1 nm) immersed in a solvent formed by particles of atomic size. The fact that they are considerably larger than particles in atomic systems makes experimental investigations much easier, using modern tools such as video microscopy or optical tweezers (for a recent overview see [1]). Further, by suitable modifications of the solvent and/or by systematic synthesis of the aggregates (see, for example, recent progress for dendrimers [2]), the physical properties of the mesoscopic particles can be tailored at will, which brings a direct comparison between theory and experiment within reach.

Since typical soft matter particles are themselves complex aggregates built up from several thousands of atoms or molecules, it is impossible to use potentials in theoretical investigations that take explicitly into account all the degrees of freedom of the constituent particles. Coarse graining methods have turned out to be a powerful tool to cope with this problem [3]; using suitable averaging procedures, these approaches drastically reduce the huge number of degrees of freedom and one finally arrives at effective (pair) interactions $\Phi(r)$: they depend typically on the distance between the centers of mass of the aggregates and thus represent potentials between artificial, "effective" particles. For a few soft matter systems such effective interactions have been proposed or derived in literature, sometimes even in closed, analytical forms: neutral and charged star polymers and microgels [4,5] are a few examples (for an overview we refer to [3]).

In contrast to atomic systems where the interatomic potentials are harshly repulsive at short distances, the effective potentials of soft matter systems show completely new features: as a consequence of a complex internal structure of the mesoscopic aggregates these particles are allowed to overlap, to mutually penetrate, or to even interweave when being compressed, which is expressed by the fact that frequently the effective potentials only weakly diverge or even remain finite at the origin. These particular features lead, in turn, to unexpected, surprising effects both in their structural properties as well as in their phase behaviour: for example, the structure factor of star polymers shows an anomalous behaviour upon compression, which is reflected in a decrease of the height of the main peak for densities larger than the overlap density [6]; in the phase diagram of these polymers and charged microgels, new and completely unexpected features were encountered such as re-entrant melting processes or clustering transitions [7,8]. In addition, well-established criteria that indicate the onset of a freezing transition in atomic systems (such as freezing criteria due to Hansen & Verlet or Lindeman [9]) break down completely and therefore loose their significance in soft systems.

These new and particular features have also to be taken into account from the conceptual point of view when calculating the properties of these systems: liquid state theories that were originally designed for systems with harshly repulsive potentials and have proved to be reliable there have to be thoroughly reconsidered; a straightforward extension to soft systems is not justified. Examples that justify this scepticism are, for instance, closure relations to the Ornstein-Zernike relation including the bridge function, $B(r)$: in those relations this function plays the role of an additional, effective potential. In systems with harshly repulsive interactions the particular shape of $B(r)$ was irrelevant at short distances, where the diverging potential dominates; this contributed to the justification of the universality hypothesis [10] which states that $B(r)$ can be approximated reasonably well by the bridge function of a suitably chosen hard sphere reference system. In soft systems, however, the situation is completely different: the particular shape of the bridge functions (which is now of the same order of magnitude as the potential at short distances) *is* now crucial and the universality hypothesis can no longer be maintained.

In several recent studies the properties of systems with soft potentials have been investigated using different liquid state theories [11,12], but no systematic investigations are available where the degree of softness of $\Phi(r)$ can be varied in a continuous way. In the present contribution we report on the structural and thermodynamic properties of a particular model system of soft matter, where the functional form of the interaction permits such a variation, the so-called generalized Gaussian core model with index n (GGCM-n):

$$\Phi_{\mathrm{GGCM}-n}(r) = \varepsilon \mathrm{e}^{-(r/\sigma)^n}. \tag{1}$$

ε is an energy parameter and σ represents a length scale. The potential interpolates smoothly, via the index n, between two model systems that have been widely used in literature: the Gaussian core model (GCM) is recovered for $n = 2$ while for $n \to \infty$, we obtain the penetrable sphere model (PSM). Further one can show [13], that the Fourier transform of the potential, $\tilde{\Phi}(q)$, is a positive, monotonously decaying function for $n \leqslant 2$, while for $n > 2$, $\tilde{\Phi}(q)$ can also attain negative values. These two scenarios correspond exactly to the classification introduced by Likos *et al.* [14] to distinguish between two classes of systems, the Q^+ and the $Q^\pm$ systems; upon compression these systems show a completely different behaviour: while Q^+ systems show re-entrant melting, a clustering transition is predicted for the $Q^\pm$ class. Although a detailed investigation of these phenomena would clearly exceed the limits of the present contribution we shall briefly come back to this feature in section 3.

Restricting ourselves to the liquid phase, we intend to fill the gap between the two limiting cases, the GCM and the PSM – which have already been studied in detail [11,12] – by considering the thermodynamic properties of GGCM-n for two different intermediate values of n, i.e. for $n = 4$ and $n = 10$. We use different liquid state theories and put emphasis on a critical test and revision of these frameworks and on a thorough discussion of the results, for the reasons mentioned above. To assess our results and to test the reliability of our numerical approaches we have performed computer simulations.

The paper is organized as follows: in the subsequent, theoretical section we shall present the model and briefly outline the liquid state concepts we have used to calculate the properties of the system. These will be discussed in section 3, starting with the structural properties and focusing then on the thermodynamics, including a brief outlook on further implications on the phase behaviour. The paper is closed with a summary of our findings.

2. Theory

2.1. The system

The functional form of the GGCM-n potential has been presented in (1); system parameters are the temperature T [where $\beta = (k_{\mathrm{B}}T)^{-1}$] and the number density ϱ, or, equivalently, the following reduced quantities, $\varepsilon^* = \beta\varepsilon$ and $\varrho^* = \varrho\sigma^3$. As mentioned above, for $n \to \infty$ we recover the potential of PSM, being given by

$$\Phi_{\mathrm{PSM}}(r) = \begin{cases} \varepsilon, & r \leqslant \sigma, \\ 0, & r > \sigma. \end{cases} \tag{2}$$

In figure 1 we compare the GGCM-n potentials for those n-values we consider in the present contribution along with the PSM potential.

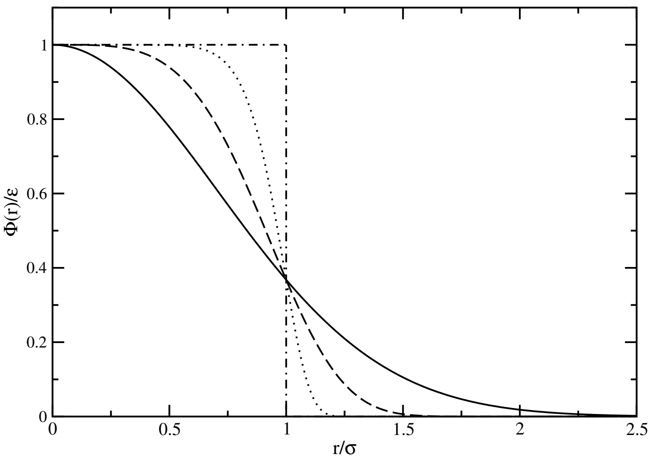

Figure 1. Potential $\Phi(r)$ of the GGCM-n as a function of r/σ [cf. (1)] for different values of n: full line – $n = 2$ (GCM), broken line – $n = 4$, dotted line – $n = 10$, and dot-dashed line – $n \to \infty$ (PSM).

2.2. Liquid state theories

We have used conventional as well as self-consistent liquid state theories to calculate the structural and thermodynamic properties of the system [9,15]. The conventional closure relations to the Ornstein-Zernike equation we have used are the hypernetted-chain (HNC) and the Percus-Yevick (PY) relations, which are given by

$$c_{\mathrm{HNC}}(r) = -\beta\Phi(r) + h(r) - \log\left[h(r) + 1\right], \tag{3}$$

$$c_{\mathrm{PY}}(r) = \left[1 - \mathrm{e}^{\beta\Phi(r)}\right] g(r) \tag{4}$$

and the mean spherical approximation (MSA), where the closure for a system with a soft potential reads

$$c_{\mathrm{MSA}}(r) = -\beta\Phi(r). \tag{5}$$

Here, $c(r)$ and $h(r)$ are the direct and the total correlation functions, and $g(r)$ is the pair distribution function (PDF). In general a numerical solution of the Ornstein-Zernike equation with one of the closure relations is required to calculate these functions. Once these functions are known, one can calculate thermodynamic properties via different thermodynamic routes. Note, however, that as a consequence of the simplifying assumptions made in their derivation, the above closure relations are only approximations of exact statistical mechanics relations; hence, the resulting correlation functions are only approximative.

The thermodynamic routes we have used to calculate the equation of state are the following [9],

$$\varrho k_{\mathrm{B}} T \kappa_{\mathrm{T}} = 1 + \varrho \int [g(\mathbf{r}) - 1]\, \mathrm{d}\mathbf{r} \quad \text{and} \quad \kappa_{\mathrm{T}} = \frac{1}{\varrho}\left(\frac{\partial P}{\partial \varrho}\right)_{\mathrm{T}}, \tag{6}$$

$$\frac{U^{\mathrm{ex}}}{N} = 2\pi\varrho \int g(r)\, \Phi(r)\, r^2\, \mathrm{d}r \quad \text{and} \quad \varrho \frac{\partial^2}{\partial \varrho^2}\left(\varrho \frac{U^{\mathrm{ex}}}{N}\right) = \frac{\partial^2}{\partial\beta\partial\varrho}\left(\varrho P^{\mathrm{ex}}\right), \tag{7}$$

$$\frac{\beta P^{\mathrm{vir}}}{\varrho} = 1 - \frac{2\pi}{3}\varrho \int r^2 \left[r\, \frac{\mathrm{d}\beta\Phi(r)}{\mathrm{d}r}\, g(r)\right] \mathrm{d}r, \tag{8}$$

where κ_{T} is the isothermal compressibility, U^{ex} and P^{ex} are the excess (over ideal gas) internal energy and pressure, and P^{vir} is the virial pressure. In the order presented above, they are called compressibility, energy, and virial routes.

If $g(r)$ were exact, then the different routes would lead to the same thermodynamic properties. However, since we obtain for $g(r)$ only approximate results, the different routes might lead to different values for a given thermodynamic property, a fact that in literature is called *thermodynamic inconsistency*. Advanced liquid state theories try to remove this deficiency by introducing more complex closure relations that enforce thermodynamic consistency between at least two different thermodynamic routes. The self-consistent liquid state theories we have used are the Zero-Separation integral-equation approach (ZSEP) [16] and the Self-Consistent Ornstein-Zernike approximation (SCOZA) ([17] and references therein). In the closure relations of these theories parameters or functions are introduced, which are chosen to enforce certain consistency relations.

The ZSEP approach is based on the following closure relation,

$$g(r) = \exp[-\beta\Phi(r) + h(r) - c(r) + B_{\mathrm{ZSEP}}(r)], \tag{9}$$

where for the bridge function $B_{\mathrm{ZSEP}}(r)$ an approximate parameterization proposed by Verlet [18] was chosen:

$$B_{\mathrm{ZSEP}}(r) = -\frac{As(r)^2}{2}\left[1 - \frac{BCs(r)}{1 + Bs(r)}\right], \tag{10}$$

$s(r) = h(r) - c(r)$ is the indirect correlation function. The parameters A, B, and C are adjusted to enforce three different self-consistency conditions: two thermodynamic relations and one structural requirement. Firstly, we require consistency between the virial and the compressibility routes, secondly, we fulfill the Gibbs-Duhem relation, and thirdly, we enforce the so-called zero separation theorem (for details see [12]). The ZSEP approach offers not only information about the structural and the thermodynamic properties. The bridge function – which plays a considerably more important role in soft matter than in the systems with harshly repulsive systems – can also be analyzed. We shall compare it with the data extracted from computer simulations.

Additionally, we report the preliminary results obtained via the SCOZA. In a straightforward generalization of the original SCOZA idea [17] the following closure to the Ornstein-Zernike relation, which can be viewed as a generalization of the MSA closure relation (5), is used:

$$c(r) = \xi(\varrho, \beta)\beta\Phi(r). \tag{11}$$

The function $\xi(\varrho, \beta)$ is chosen to enforce thermodynamic self-consistency between the compressibility and the virial routes. In conventional applications of parameterized integral-equations (such as the Rogers-Young scheme [19]), thermodynamic self-consistency was enforced only for a local state, i.e. ξ was then a simple, state-*in*dependent mixing parameter; in SCOZA, however, $\xi = \xi(\varrho, \beta)$ is explicitly state-dependent, which leads to a partial differential equation for $\xi(\varrho, \beta)$ that in general has to be solved numerically. Details will be presented in a later publication [20].

To assess our data we have performed standard Monte-Carlo simulations in a canonical ensemble [21]. Typically, around 1000 particles were used, simulations extended over 200000 sweeps and observables were averages over 20000 configurations. The usual tail corrections were applied when calculating the pressure and the energy.

3. Results

We have calculated structural and thermodynamic properties of the GGCM-n with the liquid state concepts outlined above and computer simulations, which provide reference data. For our investigations we have chosen three different n-values, $n = 2$ (i.e. the GCM), $n = 4$, and $n = 10$, and two different energy parameters for the potential, i.e., $\varepsilon^* = 0.1$ and $\varepsilon^* = 2$, for each of the three choices of n.

3.1. Structural properties

In figure 2 we display $g(r)$ for $n = 4$, $\varepsilon^* = 2$, and $\varrho^* = 2$. We observe that PY fails distinctly, and that MSA still shows some discrepancies with respect to the simulation data, in particular at short distances; HNC thus remains the only conventional liquid state theory that provides good overall agreement. Regarding the two self-consistent concepts, ZSEP and SCOZA, we observe that SCOZA slightly improves the MSA data, in particular at short distances, which can be attributed

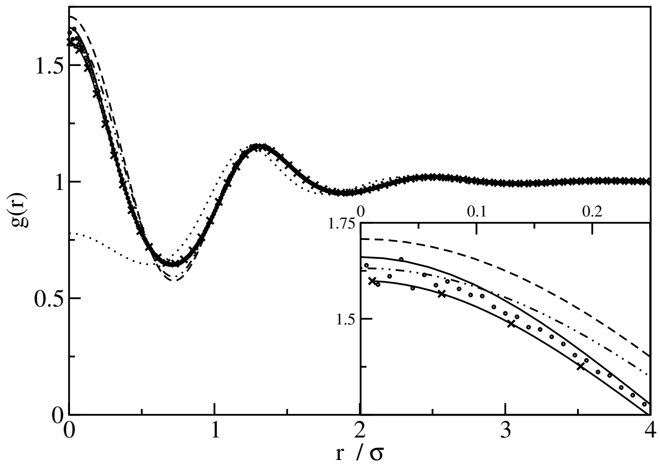

Figure 2. Pair distribution function $g(r)$ of a GGCM-n for $n = 4$ at $\varepsilon^* = 2$ and $\varrho^* = 2$. The different curves correspond to the HNC (solid line) and PY (dotted line) approximations and to the MSA (dashed line), as well as to the two self-consistent approaches considered: SCOZA (dot-dashed line) and ZSEP (solid line with crosses). The dots are the MC simulation results. In the inset a magnified view for short distances is depicted.

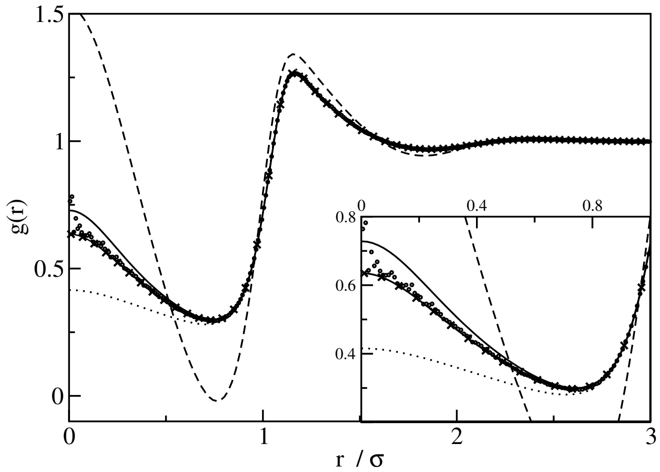

Figure 3. Pair distribution function $g(r)$ of a GGCM-n for $n = 10$ at $\varepsilon^* = 2$ and $\varrho^* = 0.5$. The labels are the same as those used in figure 2. SCOZA results are not available for this system.

to the thermodynamic self-consistency requirement; ZSEP shows perfect agreement with the simulation data. In figure 3, where we depict the results for the $g(r)$ of a GGCM-10 system at $\varepsilon^* = 2$ and $\varrho^* = 0.5$, ZSEP and Monte Carlo data agree perfectly, HNC again gives reasonable results, PY fails and MSA even goes negative. This unphysical behaviour of the MSA was already observed for the GCM [11] and there is evidence [20] that the SCOZA-PDF can also attain negative values for the GGCM-n in dependence on the system parameters. We conclude that, for soft systems, self-consistency requirements (both thermodynamic and structural) are effective concepts to provide accurate agreement with computer simulations. However, for the increasing values of n, the requirement of *thermodynamic* self-consistency alone might not be a sufficient requirement to provide physical data for $g(r)$. The requirement of the structural consistency becomes then particularly relevant (note the good agreement of ZSEP-data with simulation results for the PSM, i.e. as $n \to \infty$ [12]).

In figure 4 we display the bridge function $B(r)$ of the GGCM-4 system with $\varepsilon^* = 2$ and $\varrho^* = 2$, i.e. for a system which is considerably softer than the PSM studied in [12]. We compare $B(r)$ as predicted from the ZSEP concept and as extracted from computer simulation data (for details of the extraction procedure see [12] and references therein). The agreement is rather on a qualitative level; $B(r)$ is quite small, a fact which indicates that HNC [where $B(r) \equiv 0$] shows already a large degree of self-consistency in the sense of the ZSEP concept. At present, investigations are carried out to perform systematic studies of the bridge function in soft matter systems [22], since these functions show a behaviour which is distinctly different from the bridge functions in systems with harshly repulsive potentials.

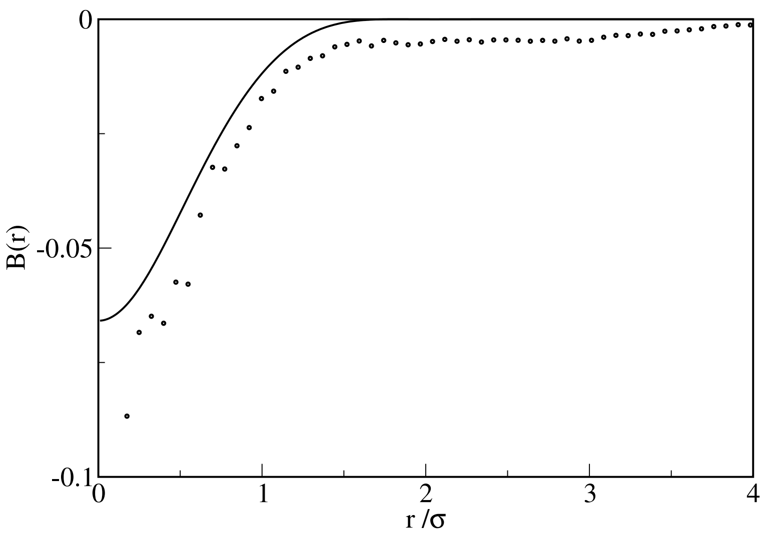

Figure 4. Bridge function $B(r)$ of a GGCM-n for $n = 4$ at $\varepsilon^* = 2$ and $\varrho^* = 2$. The solid line corresponds to the ZSEP bridge function, while the circles are the data extracted from the MC simulations.

3.2. Thermodynamic properties

In the following we present results for the dimensionless equation of state, $\beta P/\varrho$, a quantity from which one can derive via suitable relations all other thermodynamic properties of interest. We compare the results obtained via different thermodynamic routes from the liquid state theories outlined in the preceding section.

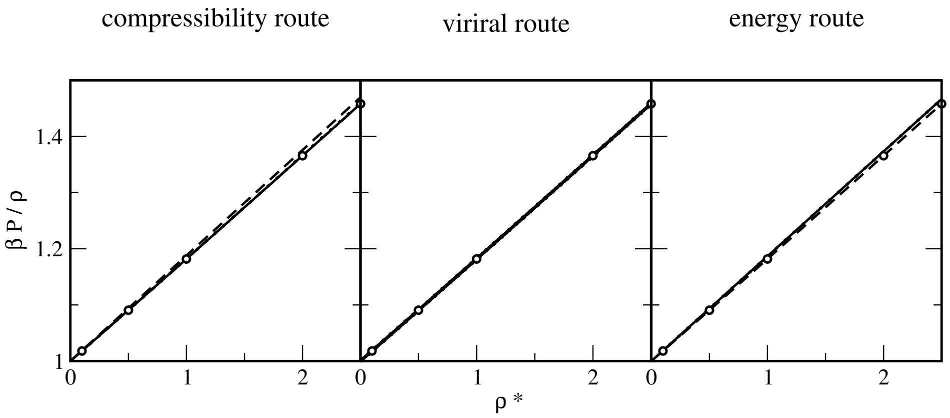

Figure 5. Dimensionless equation of state, $\beta P/\varrho$, for a GGCM-10 system as function of ϱ^* at $\varepsilon^* = 0.1$. The results provided by HNC (solid line), PY (dotted line) and ZSEP (dot-dashed line, only for the compressibility and virial routes) fall on top of each other and follow accurately the MC simulation data (circles). The MSA data (dashed line) show small discrepancies between the compressibility and energy routes.

For $\varepsilon^* = 0.1$ the situation is rather clear: independent of the thermodynamic routes, all liquid state theories provide data that are consistent within numerical accuracy and that agree well with simulation data. However, upon increasing the n-values the various liquid state theories tend to slightly deviate from the computer simulations; especially the results obtained via the compressibility and energy routes exhibit inconsistencies on the order of a few percent. We display three equations of state for $n = 10$ in figure 5.

However, as ε^* increases, differences between the theories start to emerge and the inconsistencies between the thermodynamic routes become more pronounced. From our data for $\varepsilon^* = 2$ we can conclude that the virial route generally provides the best results: not only the data from different liquid state theories coincide, but the agreement with computer simulation is very satisfactory as well. Again, as n increases, the differences between the theoretical approaches become apparent and are on the order of a few percent. The energy route performs slightly worse, in particular for large n-values, differences between the various liquid state theories emerge. In figures 6 and 7 we show the results for the energy equation for $n = 4$ and for the virial equation for $n = 10$. In contrast, the data for $\beta P/\varrho$ calculated via the compressibility route show a strong dependence on the softness of the potential (i.e. on n) and on the liquid state concept (see figure 8): we note in particular differences between PY and MSA results and computer simulation data, while the other concepts show good (HNC) or excellent agreement (ZSEP and SCOZA).

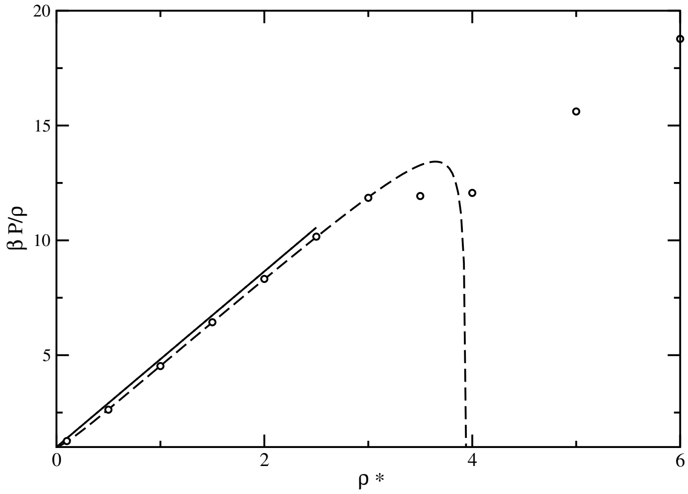

Figure 6. Dimensionless equation of state, $\beta P/\varrho$, as a function of ϱ^* at $\varepsilon^* = 2.0$, for a GGCM-4 calculated via the energy route. The labels of the curves are the same as those used in figure 5. Once again HNC, and PY data lie on top of each other and ZSEP is not depicted.

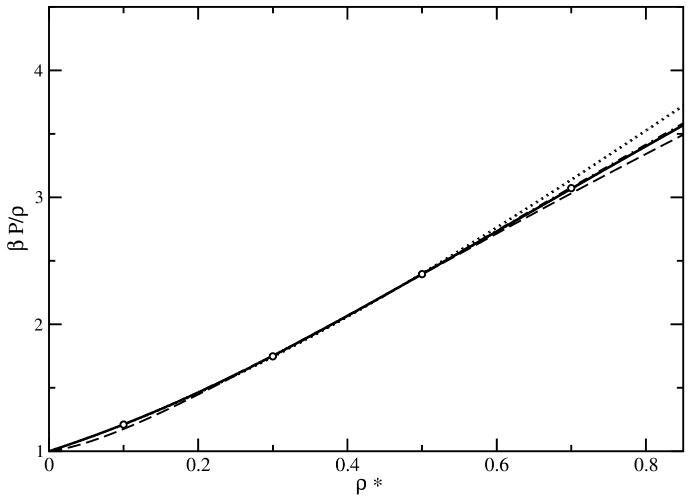

Figure 7. Dimensionless equation of state, $\beta P/\varrho$, as a function of ϱ^* at $\varepsilon^* = 2.0$, for a GGCM-10 calculated via the virial route. The labels of the curves are the same as those ones used in figure 5. Here HNC and ZSEP lie on top of each other.

Returning to figure 6, where the equation of state, calculated for $n = 4$ in computer simulations, shows a non-monotonous dependency on the number density for $\varrho^* \sim 3.5$, we also observe that none of the liquid state theories we have used has

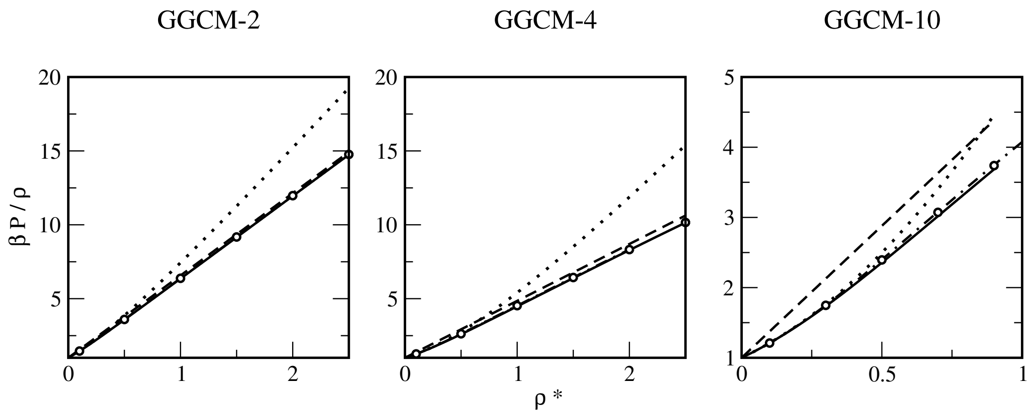

Figure 8. Dimensionless equation of state, $\beta P/\varrho$ as function of ϱ^*, for $n = 2, 4$ and 10 at $\varepsilon^* = 2$ obtained via the compressibility route. We show for the three systems the results provided by HNC, PY, MSA and ZSEP closures, as well as MC simulation data. SCOZA data are additionally shown for $n = 2$ and $n = 4$, falling on top of HNC and ZSEP in both cases. The labels correspond to the ones used in the previous figures of this section.

been capable of reproducing – not even in a qualitative way – this particular behaviour. The shape of the curve indicates the onset of a phase transition; since the GGCM-4 belongs to the $Q^{\pm}$ class [14], the observed effect is obviously a precursor of a clustering transition. An indication for the onset of such a transition can also be seen in figure 2, where the main peak of $g(r)$ has shifted to $r = 0$, suggesting that clusters with the density higher than the bulk value start to be formed. Preliminary computer simulations have shown that for higher densities clusters are indeed formed, which appear to arrange themselves on a regular lattice [13]. Further details on this phenomenon will be reported separately [23].

4. Conclusions

In this contribution we have investigated the structure and thermodynamic properties of the GGCM-n; the index n permits a interpolation between the GCM ($n = 2$) and the PSM ($n \to \infty$), and thus controls the steepness of the repulsion. For the present study we have chosen the values 2, 4, and 10 for n. The liquid state methods we have used are conventional concepts (i.e. the PY, and the HNC approximations, and the MSA) or self-consistent theories (i.e. the ZSEP approach and SCOZA), while complementary Monte Carlo simulations provide reference data. Both from the structural and thermodynamic results we can conclude that the requirement of self-consistency is a very important issue also in soft systems, which guarantees an improved agreement with simulation data. Closer investigations indicate in addition that it is in particular the requirement of structural consistency (which is expressed via the zero-separation theorem) that provides excellent results; SCOZA, on the other hand, which is based purely on thermodynamic consistency, yields for certain system parameters negative, i.e. unphysical, pair distribution functions. As we vary the index n and the energy parameter ε of the potential out of the thermodynamic routes chosen in our study, the virial route shows the best agreement with simulation data; the energy route performs slightly worse and the compressibility route often fails. In our computer simulation study of the dimensionless equation of state, $\beta P/\varrho$, we find for the GGCM-4 a non-monotonic behaviour as the density is increased: such a variation usually indicates the onset of a phase transition. In our case, we expect a clustering transition: upon compression, the particles start to form clusters, which themselves are located on a regular lattice. Further investigations of these preliminary results will be presented elsewhere.

Acknowledgements

The authors are indebted to Dieter Gottwald for numerical help and for critical comments on the manuscript. This work was supported by the Österreichische Forschungsfonds under Project Nos. P15758, and P17823: Financial support by the Hochschuljubiläumsstiftung der Stadt Wien under Proj. No. H–1080/2002 is gratefully acknowledged. BMM gratefully acknowledges financial support of the Erwin Schrödinger International Institute for Mathematical Physics, Vienna, where part of this work was carried out. MJF thanks the Instituto de Química-Física *Rocasolano* (CSIC, Spain) for providing computing resources and the Ministerio de Educación y Ciencia de España for financial support.

References

1. Special Issue dedicated to the Colloidal dispersions in external fields conference. J. Phys.-Condens. Mat., 2004, **16**, No. 38, S3769–4242.
2. Ballauf M., Likos C.N., Angew. Chem. Int. Edit., 2004, **43**, 2998–3020.
3. Likos C.N., Phys. Rep., 2001, **348**, No. 4–5, 267–439.
4. Likos C.N. *et al.*, Phys. Rev. Lett., 1998, **80**, No. 20, 4450–4453.
5. Denton A.R., Phys. Rev. E, 2003, **67**, 011804–1-10; *ibid.*, **68**, 049904(E).
6. Watzlawek M., Löwen H., Likos C.N., J. Phys.-Condens. Mat., 1998, **10**, No. 37, 8189–8205.
7. Watzlawek M., Likos C.N., Löwen H., Phys. Rev. Lett., 2002, **82**, No. 26, 5289–5292.; Likos C.N. *et al.*, J. Phys.-Condens. Mat., 2002, **14**, No. 33, 7681–7698.
8. Gottwald D. *et al.*, Phys. Rev. Lett., 2004, **92**, No. 6, 068301–1–4; Gottwald D. *et al.*, submitted to Journal of Chemical Physics, 2004.
9. Hansen J.P., McDonald I.R. Theory of Simple Liquids. Academic Press, London, 1986.
10. Rosenfeld Y., Ashcroft N.W., Phys. Rev. A, 1979, **20**, No. 3, 1208–1235.
11. Louis A.A., Bolhuis P.G., Hansen J.P., Phys. Rev. E, 2000, **62**, No. 6, 7961–7972; Lang A. *et al.*, J. Phys.-Condens. Mat., 2000, **12**, No. 24, 5087–5108.
12. Fernaud M.J., Lomba E., Lee L.L., J. Chem. Phys., 1999, **112**, No. 2, 810–816.

13. Mladek B.M. Integral Equation Theories and Computer Simulations for Systems with Bounded Potentials. Diploma Thesis, 2004, http://stud3.tuwien.ac.at/∼e9806245/diplomarbeit.pdf.
14. Likos C.N. *et al.*, Phys. Rev. E, 2001, **63**, 031206–1–9.
15. Caccamo C., Phys. Rep., 1996, **274**, No. 1, 2, 1–105.
16. Lee L.L., J. Chem. Phys., 1995, **103**, No. 21, 9388–9396.
17. Pini D., Stell G., Wilding N.B., Mol. Phys., 1998, **95**, No. 3, 483–494.
18. Verlet L., Mol. Phys., 1980, **41**, 183–192.
19. Rogers F.J., Young D.A., Phys. Rev. A, 1984, **30**, No. 2, 999–1007.
20. Mladek B.M., Kahl G., Neumann M., to be published.
21. Frenkel D., Smit B. Understanding Molecular Simulation. Computational Science Series Volume 1. Academic Press, Second Edition, 2002.
22. Fernaud M.J., Mladek B.M., Kahl G., Neumann M., to be published.
23. Mladek B.M., Gottwald D., Kahl G., Neumann M., Likos C.N., to be published.

До термодинамічних властивостей узагальненої моделі гаусового кора

Б.М.Младек [1,2], М.Д.Ферно [1], Г.Каль [1], М.Нойман [2]

[1] Центр комп'ютерного моделювання матеріалів
та Інститут теоретичної фізики
Віденського технічного університету ,
Відень, Австрія

[2] Інститут експериментальної фізики
Віденського університету,
Відень, Австрія

Отримано 24 листопада 2004 р.

Ми представляємо результати системного дослідження властивостей узагальненої моделі гаусового кора з індексом n. Потенціал такої системи з допомогою індексу n, що визначає крутизну притягання, дозволяє інтерполювати взаємодії від моделі гаусового кора до системи проникних сфер. Для розрахунку структурних і термодинамічних властивостей нами використовувалися як традиційні, так і самоузгоджені версії теорії рідкого стану, а система відліку бралася з комп'ютерного експерименту. Результати показують, що для отримання доброго узгодження з даними моделювання концепція самоузгодження стає обов'язковою; зокрема структурне узгодження, яке у нашому підході проводиться через теорему нульового розділення, є надзвичайно важливою вимогою. Результати моделювання для обезрозміреного рівняння стану, $\beta P/\varrho$, вказують на те, що для моделі з індексом 4 може виникати структурно впорядкована фаза (перехід кластерування) при стисканні системи.

Ключові слова: *м'яка речовина, інтегральні рівняння, комп'ютерне моделювання, перехід кластерування, модель гаусового кора*

PACS: *61.20.Gy, 61.20.Ja, 64.10.+h*